The Canadian Mineralogist
Vol. 40, pp. 33-46 (2002)

PHASE SEPARATION IN $(Fe,Co)_{1-x}S$ MONOSULFIDE SOLID-SOLUTION BELOW 450°C, WITH CONSEQUENCES FOR COEXISTING PYRRHOTITE AND PENTLANDITE IN MAGMATIC SULFIDE DEPOSITS

SHANNON P. FARRELL[§] AND MICHAEL E. FLEET

Department of Earth Sciences, University of Western Ontario, London, Ontario N6A 5B7, Canada

ABSTRACT

Phase relations for $(Fe,Co)_{1-x}S$ coexisting with cobalt pentlandite have been studied up to 450°C using sealed silica glass tube experiments. The (Fe,Co) monosulfide solid-solution with the NiAs-type structure (Fe,Co-*mss*) unmixes abruptly below 425°C, to coexisting Fe-rich (Fe,Co-*mss*1; 1C structure) and Co-rich (Fe,Co-*mss*2; 3C structure) phases. For bulk compositions with 52.0 at.% S, the equilibrium Fe,Co-*mss*1 solvus is located at about 0.83 molar Fe/(Fe + Co) at 400°C and progressively diverges toward the $Fe_{1-x}S$ end-member composition with decrease in temperature to 0.98 molar Fe/(Fe + Co) at 105°C. At 400°C, the equilibrium Fe,Co-*mss*2 solvus is at about 0.37 molar Fe/(Fe + Co) and does not appear to vary significantly with decrease in temperature. There is a metastable solvus within the equilibrium miscibility-gap, with a critical temperature at 425°C between 0.45 and 0.50 molar Fe/(Fe + Co), as indicated by single-phase products that persist even with prolonged annealing. A narrow field of spontaneous phase-separation is centered at 0.75 molar Fe/(Fe + Co), and results in satellite reflections of *h*0*l* NiAs-type subcell reflections in products quenched from a high temperature (800°C). The miscibility gap in Fe,Co-*mss* is similar to the phase separation of *mss* in the system Fe–Ni–S. However, phase separation occurs at a slightly higher temperature in Fe,Co-*mss* (between 425 and 400°C) than in *mss* (between 400 and 300°C), and is initially discontinuous.

Keywords: monosulfide solid-solution, phase relations, sulfide, system Fe–Co–S, cobalt pentlandite, magmatic sulfides.

SOMMAIRE

Nous avons étudié les relations de phases représentant $(Fe,Co)_{1-x}S$ en coexistance avec la cobalte pentlandite jusqu'à 450°C par expériences avec des tubes de silice scellés. La solution solide monosulfurée (Fe,Co-*mss*), possédant une structure de type NiAs, subit une démixion abruptement à une température inférieure à 425°C, pour donner un membre riche en fer (Fe,Co-*mss*1; structure 1C) et un membre riche en Co (Fe,Co-*mss*2; structure 3C). Pour des compositions globales avec 52.0% S (proportion atomique), le solvus à l'équilibre pour Fe,Co-*mss*1 se situe à un rapport Fe/(Fe + Co) d'environ 0.83 (base molaire) à 400°C et diverge progressivement vers le pôle $Fe_{1-x}S$ à mesure que diminue la température jusqu'à Fe/(Fe + Co) égal à 0.98 à 105°C. A 400°C, le solvus à l'équilibre pour la phase Fe,Co-*mss*2 se situe à un rapport Fe/(Fe + Co) d'environ 0.37 et ne semble pas varier de façon importante avec la température. Il y a un solvus métastable à l'intérieur de la lacune de miscibilité stable, avec une température critique à 425°C à une valeur de Fe/(Fe + Co) entre 0.45 et 0.50, comme l'indique la formation de produits monophasés qui perdurent malgré une cuisson prolongée. Un champ étroit de séparation spontanée des phases est centré sur un rapport Fe/(Fe + Co) de 0.75, et mène à la présence de réflexions satellites *h*0*l* par rapport à la maille de type NiAs dans les produits trempés d'une température élevée (800°C). La lacune de miscibilité pour Fe,Co-*mss* est semblable celle pour le *mss* dans le système Fe–Ni–S. Toutefois, la séparation des phases paraît à une température légèrement plus élevée dans la cas de Fe,Co-*mss* (entre 425 et 400°C) que pour *mss* (entre 400 et 300°C), et semble discontinue au départ.

(Traduit par la Rédaction)

Mots-clés: solution solide monosulfurée, relations de phases, sulfures, système Fe–Co–S, cobalte pentlandite, sulfures magmatiques.

§ *E-mail address*: sfarrele@uwo.ca

INTRODUCTION

A variety of temperature-dependent crystallographic and magnetic structural phase-transitions occur abruptly in *mss* and end-member nonstoichiometric $Fe_{1-x}S$ above 100–200°C (Power & Fine 1976, Kruse 1992). In seemingly unrelated research, Fleet (1968) found that the variation of hexagonal *a* and *c* unit-cell parameters (and d_{102} value) with composition is discontinuous as nonstoichiometric $Fe_{1-x}S$ is quenched from 700°C (see also Kruse 1990). A prominent discontinuity at 48.8 at.% Fe delineates a composition field near stoichiometric FeS that quenches to the troilite structure, with the Fe atoms forming triangular clusters (Bertaut 1953), from a field of lower Fe content in which there are now sufficient vacancies at Fe sites for ordering of vacancies to dominate the structural change on quenching (*e.g.*, Fleet 1971). The position of this discontinuity broadly corresponds to the minimum stability (at 80°C and 48.4 at.% Fe) of the field of $Fe_{1-x}S$ with the NiAs-type subcell structure, which forms a wedge between the low-temperature fields of troilite and the hexagonal pyrrhotite superstructures in the binary Fe–S phase diagram (Kissin & Scott 1982).

The present study arose from an investigation by S *K*-edge X-ray absorption near-edge structure (XANES) spectroscopy of the local electronic structure in complex monosulfide solid-solution [$(Fe,Co,Ni)_{0.923}S$] quenched from 800°C (Farrell & Fleet 2001). In that study, diffuse-intensity satellite reflections of *h0l* NiAs-type subcell reflections of Fe-rich $(Fe,Co)_{0.923}S$ compositions [near $(Fe_{0.75\times0.923\,=\,0.692}Co_{0.25\times0.923\,=\,0.231})_{\Sigma0.923}S$] indicated spontaneous phase-separation on quenching. The powder X-ray diffraction pattern of quenched $(Fe_{0.692}Co_{0.231})_{\Sigma0.923}S$ suggested some similarity to "anomalous" pyrrhotite (Fleet 1982). However, the high-2θ satellite of *h0l* subcell reflections appeared to represent relatively Co-rich Fe,Co-*mss*, whereas the low-2θ satellite correspondingly appeared to represent Fe-rich Fe,Co-*mss*. Hence, the satellite reflections of quenched $(Fe_{0.692}\ Co_{0.231})_{\Sigma0.923}S$ may indicate incipient phase-separation on quenching. We presently use powder X-ray diffraction (P–XRD) to delineate the miscibility gap in (Fe,Co) monosulfide solid-solution (Fe,Co-*mss*), and show that the phase separation is broadly similar to that of *mss* in the Fe–Ni–S system, but the unmixing continues at room temperature, with the Fe-rich solvus limb (Fe,Co-*mss*1) closely approaching the $Fe_{1-x}S$ end-member composition.

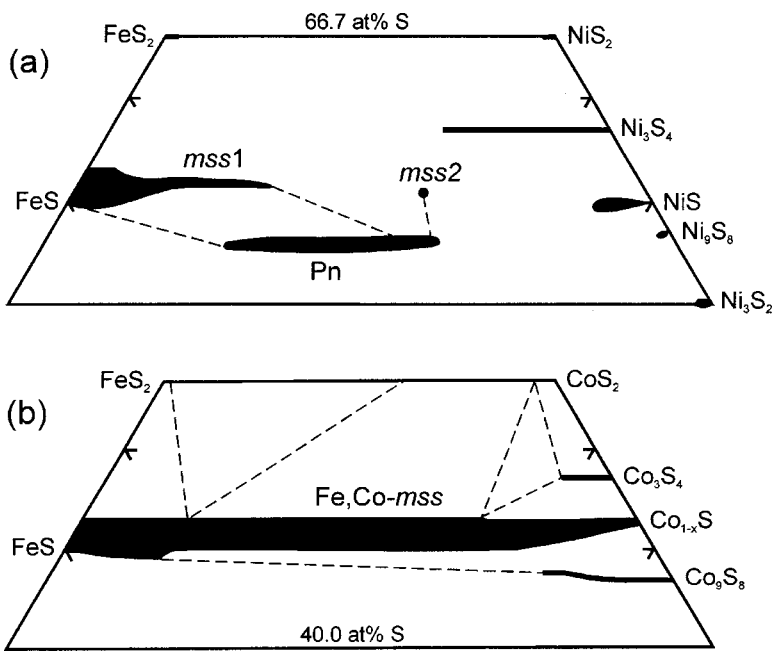

FIG. 1. Partial phase-relations at low temperature for monosulfide solid-solution (*mss*) with derivative NiAs-type structure in: (a) the system Fe–Ni–S at 230°C (after Misra & Fleet 1973, Fleet 1988), and (b) the system Fe–Co–S at 500°C (after Raghavan 1988); Pn is pentlandite.

Previous Research

NiAs-type phases

Magmatic sulfide assemblages principally consist of pyrrhotite, chalcopyrite and pentlandite. At high subsolidus temperatures, pyrrhotite and pentlandite are represented by (Fe,Ni) monosulfide solid-solution (*mss*). Low-temperature phase relations in the *mss* region of the system Fe–Ni–S were investigated by Misra & Fleet (1973) and Craig (1973). Misra & Fleet (1973) reported that *mss* is continuous between $Fe_{1-x}S$ and $Ni_{1-x}S$ to below 400°C, but is discontinuous at 300°C, with a region of solid-solution extending from $Fe_{1-x}S$ to about 25 at.% Ni (*mss*1), a second *mss* phase (*mss*2) at about 33 at.% Ni, and millerite solid-solution containing about 5 at.% Fe. At 230°C, the composition of *mss2* had not changed appreciably, but the maximum Ni content of *mss*1 had diminished to 17 at.% (Fig. 1). Craig's (1973) results are similar, except that he found the critical temperature for unmixing to be between 300 and 250°C. Misra & Fleet (1973) noted a remarkable feature: the Ni content near the *mss*1 solvus at 230°C is still appreciably greater than the range in Ni content of 0.2–0.7 at.% for intergrown hexagonal and monoclinic pyrrhotite coexisting with pentlandite in magmatic sulfides. These findings suggest that either there is a discontinuous change from *mss*1 to pyrrhotite at some lower temperature or progressive chemical readjustments in magmatic sulfides persist to very low temperatures.

The structures of *mss*, Fe,Co-*mss*, troilite, hexagonal and monoclinic pyrrhotites and jaipurite (δ-$Co_{1-x}S$) are based on the NiAs-type (B8) structure. The literature on the structure, phase relations (particularly the low-temperature non-metal – metal phase-transition), physical properties and mineralogy of NiAs-type phases is very extensive (*e.g.*, Ward 1970, Craig & Scott 1974, Morimoto *et al.* 1975a, b, Power & Fine 1976, Vaughan & Craig 1978, Kissin & Scott 1982, Anzai 1997, Raybaud *et al.* 1997, Hobbs & Hafner 1999, Farrell & Fleet 2001). This brief review is limited to a definition of terms used in describing the present phase-relations. The NiAs-type structure has S in hexagonal closest packing, metal atoms in sixfold octahedral coordination with S, and S in sixfold trigonal prismatic coordination with metal atoms. A key feature of this structure is the sharing of faces of the MS_6 (*M* is metal) octahedron along the *c*-axis direction, which permits both a direct *M*–*M* interaction *via* either metal $3d(t_{2g})$ or metal $3d(e_g)$ orbitals and an indirect *M*–S–*M* interaction *via* hybridized S 3*p* (or S 3*d*) and metal $3d(e_g)$ orbitals. The unit cell contains two formula units of *M*S. A phase with this subcell structure is presently referred to as "1C" (Vaughan & Craig 1978, Kruse 1990). Superstructure phases arise by the clustering of metal atoms in the troilite structure and the ordering of metal atoms and vacancies in more metal-deficient compositions. In the Fe–S system, troilite forms spontaneously on cooling below 147°C at the stoichiometric composition (FeS) by the triangular clustering of Fe atoms (Bertaut 1953), giving a hexagonal unit cell with $a = A\sqrt{3}$, $c = 2C$, relative to the NiAs-type subcell parameters A and C. This is presently referred to as the "2C" phase. There appear to be numerous low-temperature superstructures based on the commensurate and incommensurate ordering of Fe atoms and vacancies. Most of these superstructures have a unit cell with $a = 2A$, or an incommensurate modulation of 2A, and various patterns of order in the *c*-axis direction, giving the "nC" superstructure phases. Only structures with the ideal Fe_7S_8 composition have been determined with any detail, *e.g.*, hexagonal 3C (Fleet 1971) and monoclinic 4C (Tokonami *et al.* 1972). The 2C and hexagonal nC phases are antiferromagnetic (Schwarz & Vaughan 1972), monoclinic 4C is ferrimagnetic (Nakazawa & Morimoto 1971), and high-temperature 1C is paramagnetic (*e.g.*, Vaughan & Craig 1978, Kruse 1990). Magnetic ordering (Néel temperature) and ordering of vacancies in $Fe_{1-x}S$ both occur near 250–300°C (Power & Fine 1976) on cooling, but these ordering events are clearly composition-dependent, and details about them remain obscure (*e.g.*, Li & Franzen 1996). Hysteresis of magnetic and electrical properties and in the behavior of phase transitions and transformation is commonly encountered in heating–cooling experiments of nonstoichiometric compositions (Nakazawa & Morimoto 1971, Schwarz & Vaughan 1972, McCammon & Price 1982), but Li & Franzen (1996) attributed this to loss of S above 550°C. Finally, Fleet (1982) found that S-rich $Fe_{1-x}S$ compositions spontaneously precipitate smythite ($Fe_{13}S_{16}$) and monoclinic Fe_3S_4 when quenched from the pyrrhotite solvus and just above pyrite decomposition (743°C).

The system Fe–Co–S

There has been fairly extensive study of the low-pressure phase-relations and physical properties in the systems Fe–Co–S and Co–S (*e.g.*, Rau 1976, Wyszomirski 1976, 1977, Terukov *et al.* 1981, McCammon & Price 1982, Wieser *et al.* 1982, Barthelemy & Carcaly 1987, Collin *et al.* 1987, Raghavan 1988, Vlach 1988). Rau (1976) reviewed the binary phase-relations in the system Co–S, and showed that $Co_{1-x}S$ is stable down to only 474°C, being replaced at lower temperature by the assemblage cobalt pentlandite + Co_3S_4. Below 1058°C, the bulk composition CoS yields cobalt pentlandite + $Co_{1-x}S$ to 474°C, and cobalt pentlandite + Co_3S_4 below 474°C. Incidentally, Wyszomirski (1976) considered the existence of jaipurite, the mineral of ideal composition $Co_{1-x}S$, to be doubtful. Fe,Co-*mss* is continuous between $Fe_{1-x}S$ and $Co_{1-x}S$ down to at least 500°C, the lowest temperature investigated (Wyszomirski 1976, Raghavan 1988, present Fig. 1b). Of interest here are the following: (1) the range of *x* in $Co_{1-x}S$ is similar to that of $Fe_{1-x}S$ and *mss;* (2) Fe,Co-*mss* near FeS composition is

metal-rich [>50 at.% (Fe,Co)], similar to the case of Fe-rich *mss* (Misra & Fleet 1973), and, (3) the composition field of cobalt pentlandite is restricted to <0.2 molar Fe/(Fe + Co). Although there is extensive solid-solution between synthetic (iron–nickel) pentlandite and cobalt pentlandite (Knop & Ibrahim 1961, Geller 1962), the Fe content of natural cobalt pentlandite is also very low in the absence of Ni. Misra & Fleet (1973) found that the Co content of natural pentlandite is highly variable, ranging from almost Co-free pentlandite with less than 0.1 at.% Co to a Fe-free pentlandite of composition $Co_{6.9}Ni_{1.3}S_8$, and a Ni-free pentlandite of composition $Co_{9.1}Fe_{0.2}S_8$.

For stoichiometric ($Fe_{1-x}Co_xS$) compositions, the phase 2C extends to about $x = 0.17$, although this compositional limit varies somewhat with heat treatment and from study to study (Terukov *et al.* 1981, Wieser *et al.* 1982, Barthelemy & Carcaly 1987, Collin *et al.* 1987). The more Co-rich compositions exhibit hysteresis of magnetic and electrical properties and phase behavior. McCammon & Price (1982) investigated the magnetic behavior of $(Fe,Co)_{1-x}S$ solid-solutions quenched from 1000°C using Mössbauer spectroscopy. Their compositions ranged from $Fe_{0.834}Co_{0.166}S_{1.053}$ to $Fe_{0.009}Co_{0.991}S_{1.148}$, and they observed an antiferromagnetic ⇌ paramagnetic transition between 0.69 and 0.50 molar Fe/(Fe + Co) at 298 K and between 0.50 and 0.16 molar Fe/(Fe + Co) at 4.2 K. Thus, Fe-rich Fe,Co-*mss* compositions are antiferromagnetic like troilite and hexagonal pyrrhotites (Schwarz & Vaughan 1972) in the system Fe–S, but Co-rich Fe,Co-*mss* compositions are paramagnetic.

Experimental

Stoichiometric FeS and CoS (a mixture of $Co_{1-x}S$ and cobalt pentlandite; Fig. 1b) were prepared from hydrogen-reduced (~900°C) high-purity Fe and Co sponge, respectively, and high-purity S, reacted within evacuated sealed silica glass tubes at 450°C overnight, followed by heating at 600°C for 1 day and then at 700°C for 2 days. Initial heating near 450°C was required to prevent failure of the reaction vessel due to the rapid rise in vapor pressure of sulfur with increase in temperature beyond the boiling point at 445°C (at 1 atm.). About 0.25 g aliquots of starting mixtures prepared from appropriate molar proportions of FeS, CoS and S (Table 1) were annealed in sealed silica glass tubes at 800°C for 2 days to ensure complete reaction, and subsequently quenched in cold water; homogeneity of the samples prepared by this method was confirmed by Farrell & Fleet (2001). The quenched charges were then placed unopened in a Thermolyne model 1500 box furnace, which reproduced set temperatures to within ±5°C, and annealed at low temperature for prescribed times (Table 1) and quenched in cold water. The experiment at 105°C was annealed in a drying oven, with the temperature monitored with a mercury thermometer. Charges of bulk composition 0.75 molar Fe/(Fe + Co) and 52 at.% S were also annealed at 700°C for 2 hours and 600°C for 2 hours (after initial heating at 700°C for 2 hours) and quenched in cold water. In additional 800°C experiments, we investigated the effect of variation in molar Fe/(Fe + Co) and S content near this critical composition, and a limited number of experiments were duplicated but quenched in liquid nitrogen.

All samples were characterized by either Cu or Co*K*α X-ray powder diffraction (P–XRD) at room temperature, with minimal grinding of the samples and exposure to air. A Rigaku DMAX–II diffractometer with a horizontal goniometer and Cu*K*α X-radiation (λ = 1.5419 Å) was employed throughout an angular range of 5 to 65° (2θ), with a step size of 0.05° (2θ). For P–

TABLE 1. STARTING COMPOSITIONS, EXPERIMENTAL CONDITIONS, AND RELATIVE PROPORTION OF PHASES FOR THE (Fe–Co) MONOSULFIDE SOLID-SOLUTION (Fe,Co-*mss*; $M_{1-x}S$)

sample #	starting composition		experimental conditions		products (wt%)		
	Fe/(Fe + Co) molar	S at.%	T °C	time days	Co-rich pent-landite	Fe,Co-*mss*1 (1C)	Fe,Co-*mss*2 (3C)
00-73	0.750	51.9	425	7	0	100	0
00-74	0.562	51.9	425	7	4	96	0
00-75	0.499	52.0	425	7	6	0	94
00-76	0.453	52.0	425	7	8	0	92
00-77	0.390	52.0	425	7	9	0	91
00-65	0.750	52.0	400	7	2	87	10
00-66	0.625	52.0	400	7	3	97	0
00-67	0.563	52.0	400	7	5	95	0
00-68	0.500	52.0	400	7	17	21	62
00-72	0.453	52.0	400	7	20	13	67
00-70	0.391	52.0	400	7	13	0	87
00-71	0.313	52.0	400	7	20	0	80
00-69	0.251	52.0	400	7	22	0	79
00-53	0.687	52.0	375	7	3	97	0
00-52	0.625	52.0	375	7	6	94	0
00-51	0.563	52.0	375	7	10	52	38
00-17[1]	0.750	52.0	350	7	5	95	0
00-55	0.688	52.0	350	7	8	74	18
00-56	0.563	52.0	350	7	13	36	51
00-57	0.500	52.0	350	7	17	17	66
00-58	0.453	52.0	350	7	23	9	69
00-59	0.422	52.0	350	7	21	0	79
00-60	0.391	52.0	350	7	19	0	81
00-49	0.765	52.0	325	7	4	78	18
00-41	0.750	52.0	325	7	6	76	18
00-42	0.688	52.0	325	7	11	55	34
00-47	0.624	52.0	325	7	14	45	42
00-61	0.625	50.0	325	10	13	87	0
00-62	0.625	51.0	325	10	13	78	9
00-63	0.625	53.0	325	10	6	14	81
00-64	0.625	54.0	325	10	0	0	100
00-43	0.569	52.0	325	7	14	33	53
00-48	0.500	52.0	325	7	18	17	66
00-50	0.400	52.0	325	7	21	4	75
00-18[1]	0.750	52.0	300	7	7	70	23
00-26	0.847	52.1	250	10	4	96	0
00-12[2]	0.750	52.0	250	10	8	69	24
00-25	0.618	51.9	250	10	12	40	48
00-24	0.500	52.1	250	10	13	20	67
00-44	0.250	52.0	250	10	17	10	73
00-45	0.219	52.0	250	10	23	0	77
00-13[2]	0.750	52.0	105	28	0	100	0

[1] initial heat-treatment: 800°C for 22 hours. [2] initial heat-treatment: 800°C for 3 hours.

XRD with Co$K\alpha$ radiation [λ(Co$K\alpha_1$) = 1.7890 Å], a Rigaku X-ray diffractometer with a vertical goniometer and a Co rotating anode (45 kV, 160 mA) and equipped for automated Co$K\alpha_2$ peak removal and peak-position determination was employed throughout an angular range of 2 to 82° (2θ), with a step size of 0.02° (2θ). P–XRD patterns from the rotating anode diffractometer were not calibrated with an internal standard as done in Farrell *et al*. (in prep.). Experience has shown that the Rigaku DMAX–II diffractometer reproduces 2θ within error of measurement, and comparison of results collected using both diffractometers gave maximum discrepancies in the d_{102} reflection of only 0.001 Å.

A limited number of products were examined by X-ray precession photography (unfiltered Mo *K* radiation), single-grain Gandolfi camera P–XRD, transmission electron microscopy (TEM) and analytical scanning TEM (STEM) at the Brockhouse Institute for Materials Research, McMaster University, and by electron-probe micro-analysis (EPMA). For EPMA, we used the JEOL JXA 8600 instrument at The University of Western Ontario, operated at an accelerating voltage of 25 kV and a probe current (measured on a Faraday cup) of 30 nA. FeS and synthetic Co metal were used as standards.

Results and Discussion

Products

The variation of the d_{102} value in $(Fe,Co)_{0.923}S$ quenched from 800°C is shown in Figure 2; d_{102} increases curvilinearly from 1.948 Å in $Co_{0.923}S$ to 2.075 Å in $Fe_{0.923}S$, broadly following the trend of the *c* parameter for $Co_{1-x}S$–FeS solid-solutions quenched from 700°C (Barthelemy & Carcaly 1987). Note, however, that the discontinuity near 0.83 molar Fe/(Fe + Co) due to the 2C ⇌ 1C transition, described by Barthelemy & Carcaly (1987), is not evident in our results. This difference is due to an excess of S (~52 at.%) in the samples, which effectively excludes the 2C ⇌ 1C transition at the temperatures of investigation. Satellite reflections of *h*0*l* NiAs-type subcell reflections in P–XRD patterns of $(Fe,Co)_{0.923}S$ compositions (52.0 at.% S) quenched from 800°C are present from 0.74 to 0.81 molar Fe/(Fe + Co), and show a maximum development at Fe/(Fe + Co) = 0.75 (Figs. 3a, 4a). Some of these 800°C experiments are repeated and quenched in liquid nitrogen, but this treatment resulted in no change in the appearance of P–XRD patterns. A very slight broaden-

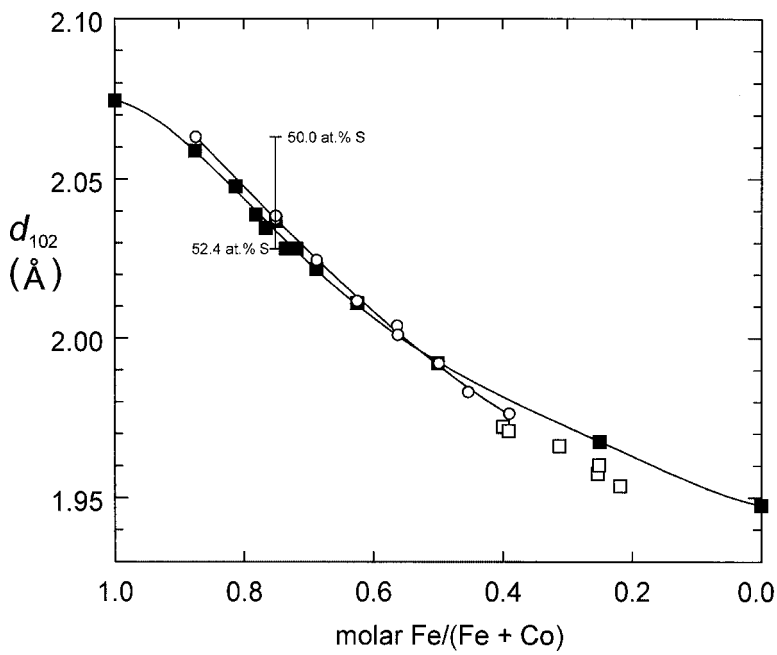

FIG. 2. Variation in the spacing d_{102} of NiAs-type subcell for $(Fe,Co)_{0.923}S$ solid solutions quenched in cold water from 800°C (full squares and vertical bar) and single-phase Fe,Co-*mss* coexisting with 0–9 wt% cobalt pentlandite (open circles) and 17–23 wt% cobalt pentlandite (squares) annealed at ≤425°C.

ing of the base of the 102 reflection is evident at Fe/(Fe + Co) = 0.72, and no anomalous scattering is present at Fe/(Fe + Co) = 0.88. Using Figure 2, it is evident that the high-2θ satellite of 102 subcell reflection represents relatively Co-rich Fe,Co-*mss*, and the low-2θ satellite represents Fe-rich Fe,Co-*mss*. Hence, the satellite reflections indicate incipient phase-separation on quenching.

With increase in Fe content at constant S content (52.0 at.%), the intensity of the 102 satellite of Fe,Co-*mss*1 becomes progressively stronger relative to that for Fe,Co-*mss*2, and achieves a maximum at Fe/(Fe + Co) = 0.75 (Fig. 3a). At constant molar Fe/(Fe + Co) (0.75), satellite reflections are not evident at 50 at.% S, have maximum development at 51.5 at.% S, and the relative

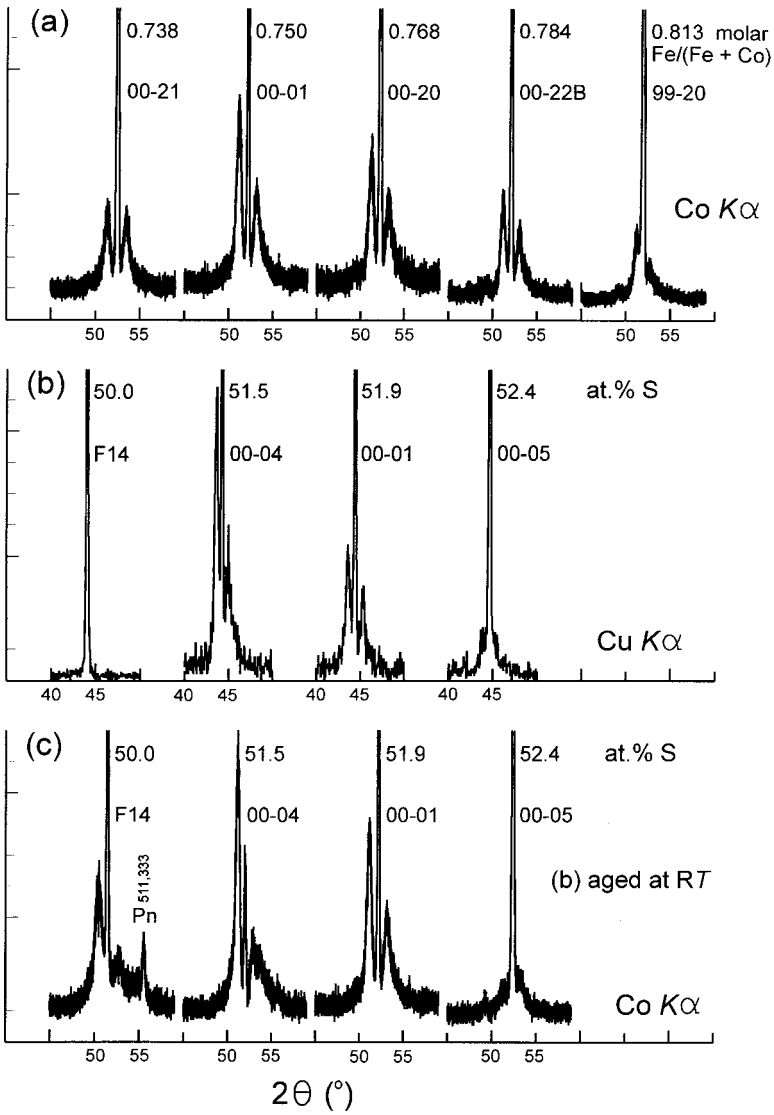

FIG. 3. Satellite reflections of 102 NiAs-type subcell reflection of $(Fe,Co)_{1-x}S$ solid solutions. (a) Series of bulk compositions with 52.0 at.% S. (b) and (c) 0.75 molar Fe/(Fe + Co); the low-2θ satellite is Fe-rich Fe,Co-*mss*1 phase, and the high-2θ satellite is Co-rich Fe,Co-*mss*2 phase. Pn is cobalt pentlandite. Experiments are quenched in cold water from 800°C. Products in part (b) are measured directly after quenching, and those in parts (a) and (c), after an interval of up to 34 months [for sample F14 in part (c)].

intensity of the 102 satellite for Fe,Co-*mss*1 diminishes relative to that for Fe,Co-*mss*2 with progressive increase in nominal S content (Fig. 3b). Charges of the bulk composition $(Fe,Co)_{0.923}S$ with Fe/(Fe + Co) = 0.75 are also annealed at and quenched from 700, 600 and 425°C, resulting in no significant change in the diffraction pattern (the P–XRD pattern shown in Fig. 4a is from the 425°C experiment). However, phase separation is complete for charges annealed at 400 and 350°C, giving an anomalous Fe-rich Fe,Co-*mss*1, and at ≤325°C giving apparently equilibrium Fe,Co-*mss*1 and Fe,Co-*mss*2 (*e.g.*, Fig. 3b; see discussion below). This sequence of experiments clearly shows that the satellite reflections develop when the quenched charges enter the miscibility gap, and that initiation of the phase-separation process is spontaneous. As described below, the miscibility gap is structured, with a metastable region immediately below the equilibrium solvus.

Interestingly, phase separation continued during storage of products at room temperature. The P–XRD patterns of Figure 3b are obtained directly after quenching, and those of Figure 3a and 3c after storage for 14 months (00–20, 00–21, 00–22B), 17 months (experiments 00–01, 00–04, 00–05), 21 months (experiment 99–20), and 34 months (experiment F14). The S-rich products (those with S ≥ 52.0 at.%) are essentially unaffected by aging. Sample 00–04, with 51.5 at.% S and showing maximum development of satellites when measured directly after quenching, is largely unmixed and has a trace of exsolved cobalt pentlandite, and sample F14, with 50.0 at.% S and showing no development of satellites directly after quenching, is extensively unmixed and has a significant amount of exsolved cobalt pentlandite (Fig. 3c).

At temperatures directly above the metastable solvus, the quenched products are single-phase Fe,Co-

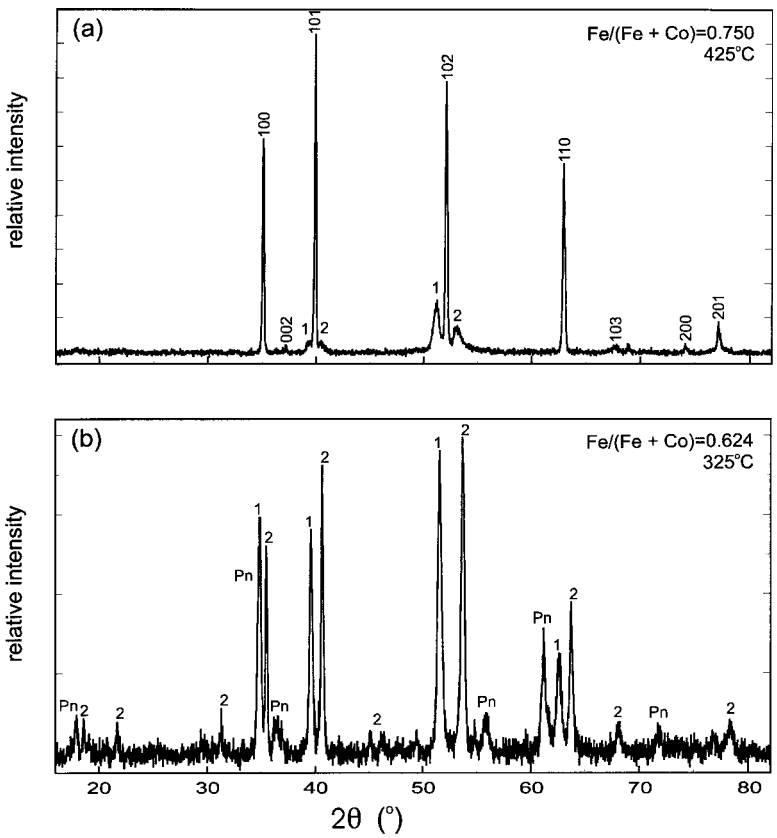

FIG. 4. P–XRD patterns: (a) Fe,Co-*mss* with satellite reflections (see Fig. 3a) quenched from 425°C (NiAs-type subcell reflections are indexed), and (b) coexisting Fe,Co-*mss*1 (1), Fe,Co-*mss*2 (2) and cobalt pentlandite (Pn) quenched from 325°C. Note that satellite reflections in part (a) develop into well-resolved Bragg reflections when the sample is annealed at low temperature; also, 3C superstructure reflections of the Fe,Co-*mss*2 phase are prominent in part (b).

mss and small amounts of cobalt pentlandite, which increased in proportion to a maximum content of about 20 wt% with increase in Co content and decrease in temperature (Table 1). The variation in d_{102} with $(Fe,Co)_{1-x}S$ composition for these annealed single-phase Fe,Co-*mss* products is shown in Figure 2. Evidently, in Co-rich compositions, d_{102} is somewhat lower for the low-temperature annealed products compared with the 800°C quenched products. This decrease in d_{102} is a consequence of the small increase in S content for the Fe,Co-*mss* owing to precipitation of cobalt pentlandite. However, from the variation in d_{102} with S content at molar Fe/(Fe + Co) = 0.75, these discrepancies seem to correspond to a maximum increase in S of only about 0.5 at.%. Superstructure reflections are not evident in P–XRD patterns of Fe-rich bulk compositions (*e.g.*, Fig. 4a) which, therefore, quenched as the phase 1C. P–XRD patterns of Co-rich bulk compositions are characterized by reflections of the hexagonal 3C superstructure (Fleet 1971; our Table 2), which are undetected beyond 0.50 molar Co/(Fe + Co). Thus, the 1C $\rightleftharpoons$ 3C transition occurs between 0.55 and 0.50 molar Fe/(Fe + Co) at 450–100°C and, therefore, could be related to the antiferromagnetic $\rightleftharpoons$ paramagnetic transition documented by McCammon & Price (1982) between 0.69 and 0.50 molar Fe/(Fe + Co) at 298 K and 0.50 and 0.16 molar Fe/(Fe + Co) at 4.2 K. However, McCammon & Price (1982) quenched their experiments from 1000°C, so that their Co-rich Fe,Co-*mss* products are likely 1C, whereas the present annealed products are vacancy-ordered and likely magnetically ordered as well. Conversely, the present Fe-rich Fe,Co-*mss* products are 1C and likely magnetically ordered but (apparently) not vacancy-ordered.

The metastable solvus is marked by the appearance of two-phase Fe,Co-*mss* (Fe,Co-*mss*1 + Fe,Co-*mss*2) with cobalt pentlandite. The proportion of cobalt pentlandite is estimated from the relative areas of the 440 reflection of pentlandite and sum of the 110 reflections of Fe,Co-*mss*1 and Fe,Co-*mss*2 (Fig. 4b, Table 1). A calibration curve was constructed using P–XRD data to determine the relative percentage of cobalt pentlandite, with respect to total pyrrhotite, for mixtures of synthetic Co_9S_8 and FeS in varying proportions; differential absorption effects were ignored. Cobalt pentlandite is present up to a maximum of 23 wt% in Co-rich bulk compositions; its proportion decreases systematically to 2 wt% in Fe-rich compositions, and does not seem to vary significantly with temperature from 400 to 250°C for any given bulk-composition.

TABLE 2. POWDER X-RAY-DIFFRACTION PATTERN OF THE PHASE 2A,3C [1]

hkℓ	2θ (°)	$d_{hk\ell}$ (Å)	I_{rel}	*hkℓ*	2θ (°)	$d_{hk\ell}$ (Å)	I_{rel}
1 0 1	18.48	5.571	11	3 0 0	54.43	1.956	9
1 0 2	21.54	4.787	9	2 1 4	54.63	1.949	12
1 0 4	31.08	3.339	6	3 0 2	56.09	1.903	6
2 0 0	35.38	2.944	40	2 2 0	63.57	1.698	6
1 0 5	36.74	2.838	8	3 0 5	64.47	1.677	45
2 0 3	40.51	2.584	82	2 0 9	71.26	1.535	8
1 1 5	44.87	2.344	6	1 0 11	78.12	1.420	10
2 0 6	53.46	1.989	100	4 0 3	78.40	1.415	8

[1] a 6.792(4), c 16.202(10) Å; experiment # 00-64, Fe/(Fe + Co) = 0.625 (molar), 54.0 at.% S, Co$K\alpha_1$ radiation, [λ (Co$K\alpha_1$) = 1.7890 Å].

Microstructures

X-ray precession photographs of single-crystal fragments of $(Fe,Co)_{0.923}S$ annealed below the metastable solvus show well-resolved reflections of both Fe,Co-*mss*1 and Fe,Co-*mss*2 in coherent intergrowth, with $c_{Fe,Co\text{-}mss1}^*$ // $c_{Fe,Co\text{-}mss2}^*$ and $a_{Fe,Co\text{-}mss1}^*$ // $a_{Fe,Co\text{-}mss2}^*$ (Fig. 5). However, there is too little contrast for the separate domains of Fe,Co-*mss*1 and Fe,Co-*mss*2 to be resolved in our preliminary TEM and STEM study. Back-scattered electron (BSE) EPMA was slightly more successful, but only after numerous sections of several products had been surveyed. For Fe-rich compositions, submicrometric lamellae of cobalt pentlandite are resolved in three orientations with blotchy blebs of Fe,Co-*mss*2 in a matrix of Fe,Co-*mss*1 (Fig. 6a). As described below, this is evidently a (00.1) section of Fe,Co-*mss*. Other sections normal to (00.1) reveal an indistinct parallelism of submicrometric Fe,Co-*mss*1 and Fe,Co-*mss*2 lamellae. Hence, the lamellae of Fe,Co-*mss*2 resolved in the (00.1) section, shown in Figure 6a, are lensoid in cross section, and the respective lattices are aligned in near-coincidence with Fe,Co-*mss*1 with $(00.1)_{Fe,Co\text{-}mss2}$ // $(00.1)_{Fe,Co\text{-}mss1}$. For Co-rich compositions, cobalt pentlandite tends to occur along grain contacts instead of forming submicrometric lamellae (Fig. 6b); blotchy blebs of Fe,Co-*mss*2 in a matrix of Fe,Co-*mss*1 still persist.

On the basis of the three orientations of cobalt pentlandite lamellae in the section shown in Figure 6a, the orientation of exsolved cobalt pentlandite in Fe,Co-*mss* appears to be the same as that of lamellae of pentlandite (Pn) in both natural and synthetic crystals of pyrrhotite (Po), which is $(111)_{Pn}$ // $(00.1)_{Po}$, $(011)_{Pn}$ // $(11.0)_{Po}$, and $(112)_{Pn}$ // $(10.0)_{Po}$ (Francis *et al.* 1976). Although lamellar-twinned flames of pentlandite in pyrrhotite are generally in only one of the three equivalent orientations, Ehrenberg (1932) reported that there are some sections of Sudbury magmatic sulfide ore with pentlandite in three distinct orientations resembling a snowflake, and a sample from Miggiadone bei Pallanza, Piemont, Italy, has pentlandite in three orientations epitactically overgrowing the (00.1) face of a crystal of pyrrhotite (Fig. 2 of Francis *et al.* 1976). In synthesis experiments in the system Fe–Ni–S, Francis *et al.* (1976) found that rapidly quenched samples of *mss* contain randomly oriented blebs of pentlandite, whereas slowly cooled samples contain lamellae of pentlandite parallel to (00.1) of pyrrhotite.

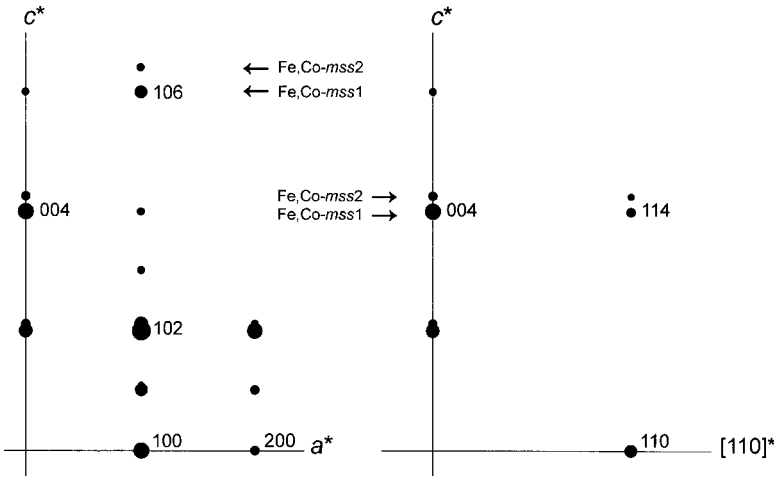

FIG. 5. Sketches of single-crystal X-ray precession photographs taken with Mo$K\alpha$ radiation of Fe,Co-*mss*1 and Fe,Co-*mss*2 in coherent lamellar intergrowth of 0.625 molar Fe/(Fe + Co), 52.0 at.% S heated at 1000°C and annealed at 325°C. Very minor radial smearing of reflections due to lamellar twinning has been ignored.

Phase relations

The products annealed below the metastable solvus are too finely intergrown for meaningful EPMA. Preliminary analysis of the phases imaged in Figure 6a indicate 39.9 at.% Fe, 8.0% Co, 52.1% S, and Fe/(Fe + Co) = 0.83 for Fe,Co-*mss*1, 29.2 at.% Fe, 18.7% Co, 52.1% S, and Fe/(Fe + Co) = 0.61 for Fe,Co-*mss*2, and 19.5 at.% Fe, 31.6% Co, 48.9% S, and Fe/(Fe + Co) = 0.38 for cobalt pentlandite, respectively, but these compositions are clearly contaminated by beam overlap and fluorescence excitation, particularly with respect to proportions of Fe and Co. The composition of cobalt pentlandite is indeterminate. Fortunately, the molar proportions of Fe and Co in coexisting Fe,Co-*mss*1 and Fe,Co-*mss*2 could be determined independently using the variation of d_{102} with composition for charges quenched from 800°C (Fig. 2). Although significant error in the estimated composition of Fe,Co-*mss*2 is anticipated owing to the large amount of exsolved cobalt pentlandite in Fe,Co-rich bulk compositions, the agreement between charges of widely different bulk-composition is quite good. In fact, the Fe,Co-*mss*2 solvus limb determined by the d_{102} method is in good agreement with that determined from phase appearance (Fig. 7). Also, for individual experiments, the molar proportion of coexisting Fe,Co-*mss*1 and Fe,Co-*mss*2 indicated by the d_{102} method is consistent with the weight proportion estimated from the relative intensity of equivalent subcell reflections (*e.g.*, 101, 102, 110) for the two phases (*cf.* Fig. 4b).

Our annealing experiments reveal that for bulk compositions with about 52.0 at.% S, a broad miscibility gap develops in Fe,Co-*mss* below 425°C (Fig. 7). The phase separation in Fe-rich Fe,Co-*mss* is complex. There is evidence of a metastable solvus with a critical temperature at 425°C between 0.45 and 0.50 molar Fe/(Fe + Co), and a narrow field of spontaneous unmixing centered at 0.75 molar Fe/(Fe + Co). However, the equilibrium Fe,Co-*mss*1 solvus at 400°C seems to be at about 0.83 molar Fe/(Fe + Co), suggesting that the solid solution likely breaks down by reaction just below 425°C. The Fe,Co-*mss*1 solvus then diverges progressively toward the $Fe_{1-x}S$ end-member with a decrease in temperature to 0.97–0.98 molar Fe/(Fe + Co) at 105°C. The equilibrium Fe,Co-*mss*2 solvus is at about 0.37 molar Fe/(Fe + Co) and does not appear to vary significantly with a decrease in temperature to 105°C. The nucleation of cobalt pentlandite is not noticeable upon the abrupt unmixing of Fe,Co-*mss* just below 425°C. Rather, the results in Table 1 show that the weight proportion of cobalt pentlandite increases progressively with increase in Co content of the bulk composition, consistent with its extremely Co-rich composition. In Figure 7, the equilibrium solvus is defined from the compositions of the unmixed annealed solid-solutions, whereas the metastable solvus is defined by single-phase products occurring between the metastable and equilibrium miscibility gaps that persist even with prolonged annealing.

In charges of bulk composition 0.75 molar Fe/(Fe + Co) annealed at 350 and 400°C, the compositions of coexisting Fe,Co-*mss*1 and Fe,Co-*mss*2 are anomalous [0.95–0.98 and 0.55 molar Fe/(Fe + Co), respectively] and inconsistent with the equilibrium solvi. This discrepancy may be understood by noting similarities between the phase separation in Fe-rich Fe,Co-*mss* and the

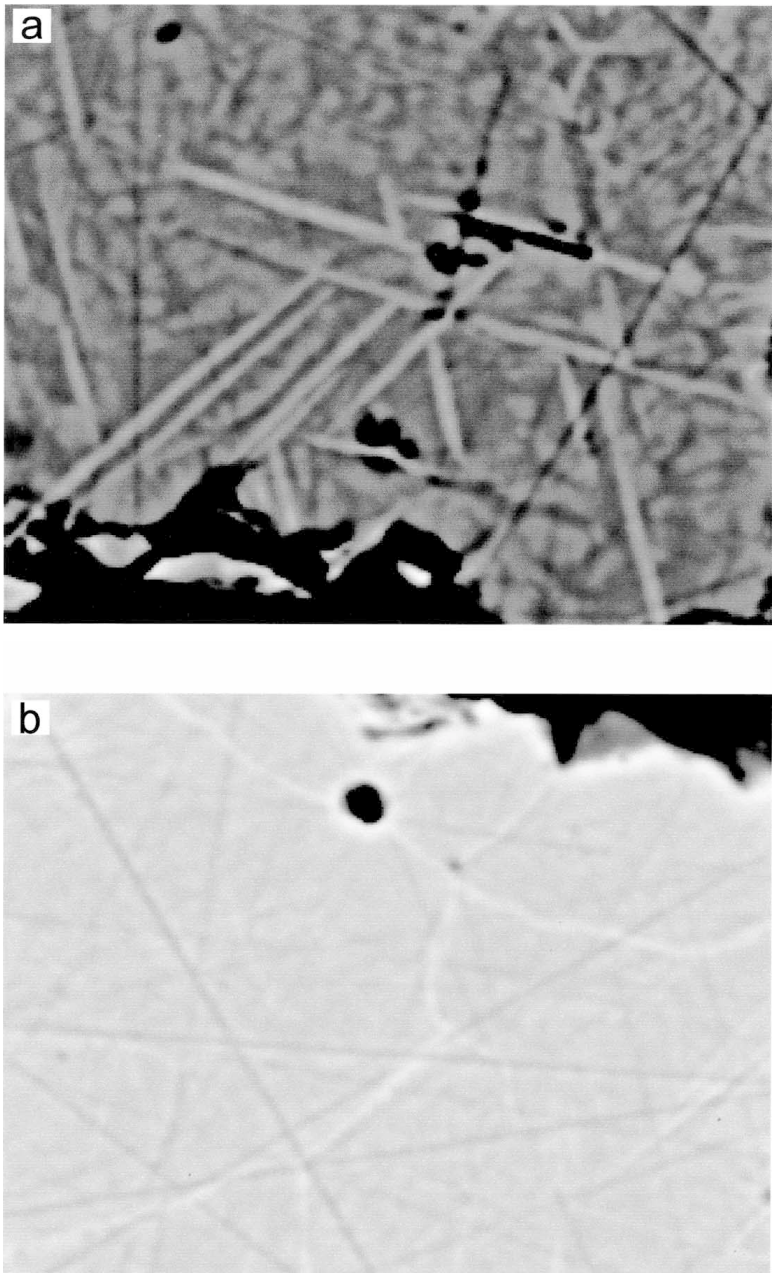

FIG. 6. EPMA BSE images of coexisting Fe,Co-*mss*1, Fe,Co-*mss*2 and cobalt pentlandite. (a) Bright lamellae in three orientations are cobalt pentlandite, light blotchy blebs are Fe,Co-*mss*2, and dark matrix is Fe,Co-*mss*1. Grain section is oriented close to (00.1) of Fe,Co-*mss* phases; experiment #00–42, 0.688 molar Fe/(Fe + Co), 52.0 at.% S, quenched from 325°C. The field of view is 45 μm wide. (b) Cobalt pentlandite lies along grain boundaries, light blotchy blebs are Fe,Co-*mss*2, and darker matrix is Fe,Co-*mss*1; experiment #00–72, 0.453 molar Fe/(Fe + Co), 52.0 at.% S, quenched from 400°C. The field of view is 35 μm wide.

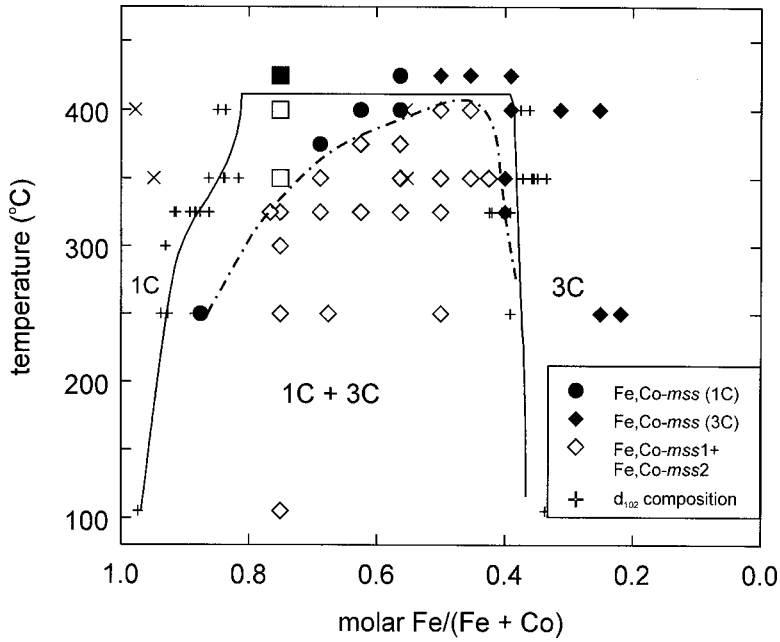

FIG. 7. Pseudobinary temperature–composition phase diagram for bulk compositions with 52.0 at.% S annealed at low temperature and quenched in cold water. The dot–dash line represents the metastable solvus, as defined by phase appearance. The full line is the equilibrium miscibility gap with limbs defined from d_{102} of unmixed solid solutions within the metastable solvus. Squares refer to experiments resulting in spontaneous decomposition (X) with metastable exsolution. Note that single-phase products are present between the metastable and equilibrium miscibility gaps and persisted even with prolonged annealing.

spinodal unmixing of alloys. Evidently, the metastable limb of the solvus represents depression of unmixing by the contribution from elastic strain energy. The ideal spinodal theory is based on a random distribution of end-member components, but the 0.75 molar Fe/(Fe + Co) composition is clearly special in respect to ordering of Fe and Co atoms. Phase separation is spontaneous below 425°C because ordering of Fe and Co relaxes the elastic strain energy. However, because separation is very rapid, equilibrium compositions are not attained. The Fe,Co-*mss*1 limb is near end-member $Fe_{1-x}S$, and the Fe,Co-*mss*2 limb compositions may be sensing the Co-rich limit of the field of the phase 1C (Fig. 7). Also, when the coexisting Fe,Co-*mss*1 and Fe,Co-*mss*2 lamellae achieve a critical size, they are not able to re-equilibrate by diffusion alone under the temperature–time conditions of the present annealing experiments.

It is difficult to estimate the S content of coexisting Fe,Co-*mss*1 and Fe,Co-*mss*2. The preliminary EPMA of the Fe,Co-*mss* phases (Fig. 6a) pertained to an area remote from cobalt pentlandite, so that the S content obtained (52.1 at.%) should be, at least, representative of a weighted average of Fe,Co-*mss*1 and Fe,Co-*mss*2. At 325°C, within the miscibility gap, exsolution of cobalt pentlandite thus has not increased the S content of the Fe,Co-*mss* significantly beyond the nominal starting composition of 52.0 at.%. A contributing factor here may be the minimal loss of S to the vapor space of the sealed silica glass tubes at 800°C, which, if it had not reacted back during the low-temperature annealing, would have shifted the effective starting compositions to slightly lower S content. However, the quantity of cobalt pentlandite in Co-rich bulk compositions is considerable (about 20 wt%; Table 1). Assuming ideal cobalt pentlandite stoichiometry and a nominal bulk S content of 52.0 at.%, precipitation of 20 wt% cobalt pentlandite would increase the S content of coexisting Fe,Co-*mss*2 to about 53.4 at.%. Recognizing that cobalt pentlandite coexisting with Fe,Co-*mss* is likely to be relatively S-rich (*cf.* Misra & Fleet 1973) and that some S is lost to the vapor phase, and in light of the preliminary EPMA results and the observation that the quantity of cobalt pentlandite exsolved is generally independent of temperature at a given bulk-composition, we

presently assume a S content of 52.5 at.% for Fe,Co-*mss*2 in this series of experiments. The S content of Fe,Co-*mss*1 seems to be close to the nominal composition of 52.0 at.%.

Schematic phase-relations in the system Fe–Co–S at 325°C (Fig. 8) have been deduced from the solvi positions for a bulk S content of 52.0 at.% (Fig. 7) and phase appearance and intensities of subcell reflections for Fe,Co-*mss*1 and Fe,Co-*mss*2 in a series of experiments made at 0.625 molar Fe/(Fe + Co) (Table 1), with some adjustment of compositions for precipitation of cobalt pentlandite. Cobalt pentlandite is added for reference and assumed to be stoichiometric M_9S_8. The field of Fe,Co-*mss*, which is continuous between $Fe_{1-x}S$ and $Co_{1-x}S$ compositions at 500°C, is restricted at 325°C for Co-rich compositions and embayed toward the S-rich boundary of the field of the low-temperature phase 1C along the join Fe–S (*cf.* Kissin & Scott 1982). Fe,Co-*mss*1 is represented by a field of the phase 1C at Fe-rich and S-poor compositions, and Fe,Co-*mss*2, by a field of the phase 3C extending from relatively Co-rich to more S-rich compositions. The Fe,Co-*mss*2 solvus limb is present down to 105°C (Fig. 7), but the extent of the phase 3C at very low temperatures is unknown. The field of phase 1C evidently recedes progressively toward the $Fe_{1-x}S$ end-member with decrease in temperature (Fig. 7). The position of the low-2θ satellite of the 102 subcell reflection of the room-temperature-aged sample with 50.0 at.% S (Fig. 3c) is consistent with an end-member $Fe_{1-x}S$ near FeS in composition. However, in Figure 8 we have not delineated the boundary surface for the 2C ⇌ 1C transition for charges quenched below 147°C. The phase 1C of Fe- and S-poor composition has too few cation vacancies for vacancy-ordering to be significant. Some association of the metal atoms into triangular clusters is no doubt present in quenched samples, but this effect is too weak to result in the overall distortion that characterizes the phase 2C. Nevertheless, the combined 2C + 1C field for the quenched phase 1C does appear to be equivalent to the field of metal-rich $Fe_{1-x}S$ indicated by the early quench-type experiments of Fleet (1968).

Comparison with coexisting pyrrhotite and pentlandite

There are clearly broad similarities between the phase separation of Fe,Co-*mss* in the system Fe–Co–S and of *mss* in the system Fe–Ni–S, with Fe,Co-*mss*2 identified with *mss*2 and Fe,Co-*mss*1 with *mss*1 of Misra & Fleet (1973). The fields of Co- and Ni-rich *mss* are restricted to special ternary compositions, because NiAs-type phases are not stable along the Co–S and Ni–S joins at low temperature. However, phase separation occurs at a slightly higher temperature in Fe,Co-*mss* (between 425 and 400°C) than in *mss* (between 400 and 300°C), and is initially discontinuous. Moreover, unmixing in Fe,Co-*mss* proceeds very rapidly; there is a narrow region of spontaneous instability centered at 0.75 molar Fe/(Fe + Co), other bulk compositions within the miscibility gap are clearly unstable if annealed for short periods, and the unmixing can be followed down to room temperature.

These differences reflect the greater covalence and metallic character of Co sulfides (and alloy compounds in general). Iron is simply more compatible with Ni than with Co in NiAs-type and pentlandite-type structures. Farrell & Fleet (2001) noted that the *c* parameter of *mss* in the quaternary system Fe–Co–Ni–S decreases progressively in the sequence $Co_{1-x}S < Ni_{1-x}S < Fe_{1-x}S$ corresponding to a progressive increase in the indirect *M*–*M* (metallic) bonding interaction in the *c*-axis direction. Increase in metallic character in the ferrous metal monosulfides shortens the *M*–S bonds and increases covalence and orbital (or band) overlap. This seems to be the explanation for the inverse correlation between *c* and the area of the edge peak in the S *K*-edge XANES spectra of $(Fe,Co,Ni)_{0.923}S$ solid solutions.

Although we have associated the Fe,Co-*mss*1 solvus limb with the phase 1C, its composition evidently shifts with decrease in temperature toward the field of intergrown hexagonal pyrrhotite and monoclinic pyrrhotite of magmatic sulfide deposits (Fig. 8). Therefore, we suggest that the reduction in Ni content from the 230°C

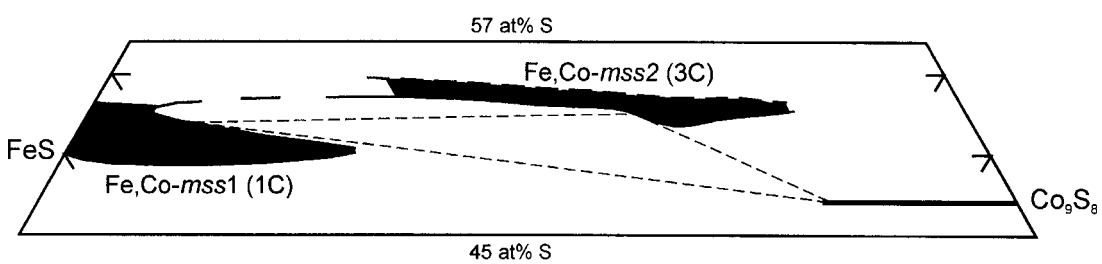

FIG. 8. Partial phase-relations of incompletely unmixed Fe,Co-*mss* in the ternary system Fe–Co–S at 325°C. Phase 1C is Fe,Co-*mss*1, and phase 3C is Fe,Co-*mss*2; note that actual extent of the cobalt pentlandite field is unknown.

*mss*1 solvus of Misra & Fleet (1973) to the very low amounts (0.2–0.7 at.%) of intergrown hexagonal pyrrhotite and monoclinic pyrrhotite coexisting with pentlandite in magmatic sulfides may have been continuous. However, recrystallization, perhaps promoted by fluids, must have continued to very low temperatures as well, because the proportion of pentlandite generally present as exsolution flames (or lamellae) in pyrrhotite is inconsistent with the required reduction in Ni content.

Acknowledgements

We thank the reviewers, J.R. Craig and P.G. Spry, for helpful comments, Kim Law for assistance with P–XRD, and Yves Thibault for assistance with EPMA. This work was supported by the Natural Sciences and Engineering Research Council of Canada. SPF is appreciative of support received from the Mineralogical Association of Canada (inaugural scholarship) and the International Centre for Diffraction Data (crystallography scholarship).

References

Anzai, S. (1997): Effect of correlations on electronic and magnetic properties of transition metal chalcogenides. *Physica* **B237**, 142-145.

Barthelemy, E. & Carcaly, C. (1987): Phase relations and ageing effects in $Fe_{1-x}Co_xS$ system. *J. Solid State Chem.* **66**, 191-203.

Bertaut, E.F. (1953): Contribution à l'étude des structures lacunaires: la pyrrhotine. *Acta Crystallogr.* **6**, 557-561.

Collin, G., Gardette, M.F. & Comes, R. (1987): The $Fe_{1-x}Co_xS$ system ($x < 0.25$); transition and the high temperature phase. *J. Phys. Chem. Solids* **48**, 791-802.

Craig, J.R. (1973): Pyrite–pentlandite assemblages and other low temperature relations in the Fe–Ni–S system. *Am. J. Sci.* **273-A**, 496-510.

_____ & Scott, S.D. (1974): Sulfide phase equilibria. *In* Sulfide Mineralogy (P.H. Ribbe, ed.). *Mineralogical Society of America, Short Course Notes* **1** CS1-100.

Ehrenberg, H. (1932): Orientierte Verwaschungen von Magnetkies und Pentlandit. *Z. Kristallogr.* **82**, 309-315.

Farrell, S.P. & Fleet, M.E. (2001) Sulfur K-edge XANES study of local electronic structure in ternary monosulfide solid solution $[(Fe,Co,Ni)_{0.923}S]$. *Phys. Chem. Solids* **28**, 17-27.

Fleet, M.E. (1968): On the lattice parameters and superstructures of pyrrhotites. *Am. Mineral.* **53**, 1846-1855.

_____ (1971): The crystal structure of a pyrrhotite (Fe_7S_8). *Acta Crystallogr.* **B27**, 1864-1867.

_____ (1982): Synthetic smythite and monoclinic Fe_3S_4. *Phys. Chem. Minerals* **8**, 241-246.

_____ (1988): Stoichiometry, structure and twinning of godlevskite and synthetic low-temperature Ni-excess nickel sulfide. *Can. Mineral.* **26**, 283-291.

Francis, C.A., Fleet, M.E., Misra, K. & Craig, J.R. (1976): Orientation of exsolved pentlandite in natural and synthetic nickeliferous pyrrhotite. *Am. Mineral.* **61**, 913-920.

Geller, S. (1962): Refinement of the crystal structure of Co_9S_8. *Acta Crystallogr.* **15**, 1195-1198.

Hobbs, D. & Hafner, J. (1999): Magnetism and magneto-structural effects in transition-metal sulphides. *J. Phys. Condens. Matter* **11**, 8197-8222.

Kissin, S.A. & Scott, S.D. (1982): Phase relations involving pyrrhotite below 350°C. *Econ. Geol.* **77**, 1739-1754.

Knop, O. & Ibrahim, M.A. (1961): Chalcogenides of the transition elements. II. Existence of the π phase in the M_9S_8 section of the system Fe–Co–Ni–S. *Can. J. Chem.* **39**, 297-317.

Kruse, O. (1990): Mössbauer and X-ray study of the effects of vacancy concentration in synthetic hexagonal pyrrhotites. *Am. Mineral.* **75**, 755-763.

_____ (1992): Phase transitions and kinetics in natural FeS measured by X-ray diffraction and Mössbauer spectroscopy at elevated temperatures. *Am. Mineral.* **77**, 391-398.

Li, F. & Franzen, H.F. (1996): Ordering, incommensuration, and phase transitions in pyrrhotite. II. A high-temperature X-ray powder diffraction and thermomagnetic study. *J. Solid State Chem.* **126**, 108-120.

McCammon, C.A. & Price, D.C. (1982): A Mössbauer effect investigation of the magnetic behaviour of $(Fe, Co)S_{1+x}$ solid solutions. *J. Phys. Chem. Solids* **43**, 431-437.

Misra, K.C. & Fleet, M.E. (1973): The chemical compositions of synthetic and natural pentlandite assemblages. *Econ. Geol.* **68**, 518-539.

Morimoto, N., Gyobu, A., Mukaiyama, H. & Izawa, E. (1975a): Crystallography and stability of pyrrhotites. *Econ. Geol.* **70**, 824-833.

_____, _____, Tsukuma, K. & Koto, K. (1975b): Superstructure and nonstoichiometry of intermediate pyrrhotite. *Am. Mineral.* **60**, 240-248.

Nakazawa, K. & Morimoto, N. (1971): Phase relations and superstructures of pyrrhotite, $Fe_{1-x}S$. *Mat. Res. Bull.* **6**, 345-358.

Power, L.F. & Fine, H.A. (1976): The iron–sulphur system. 1. The structures and physical properties of the compounds of the low-temperature phase fields. *Minerals Sci. Engng* **8**(2), 106-128.

RAGHAVAN, V. (1988): The Co–Fe–S (cobalt – iron – sulphur) system. *In* Phase Diagrams of Ternary Iron Alloys, Part 2. Indian Institute of Metals, Calcutta, India (93-106).

RAU, H. (1976): Range of homogeneity and defect energetics in $Co_{1-x}S$. *J. Phys. Chem. Solids* **37**, 931-934.

RAYBAUD, P., HAFNER, J., KRESSE, G. & TOULHOAT, H. (1997): Ab initio density functional studies of transition-metal sulphides. II. Electronic structure. *J. Phys. Condens. Matter* **9**, 11107-11140.

SCHWARZ, E.J. & VAUGHAN, D.J. (1972): Magnetic phase relations of pyrrhotite. *J. Geomag. Geoelectr.* **24**, 441-458.

TERUKOV, E.I., ROTH, S., KRABBES, G. & OPPERMANN, H. (1981): The magnetic properties of cobalt-doped iron sulphide $Fe_{1-y}Co_yS$ ($y \leq 0.13$). *Phys. Stat. Sol.* **A68**, 233-238.

TOKONAMI, M., NISHIGUCHI, K. & MORIMOTO, N. (1972): Crystal structure of a monoclinic pyrrhotite (Fe_7S_8). *Am. Mineral.* **57**, 1066-1080.

VAUGHAN, D.J. & CRAIG, J.R. (1978): *Mineral Chemistry of Metal Sulfides*. Cambridge University Press, Cambridge, U.K.

VLACH, K.C. (1988): *A Study of Sulfur Pressures and Phase Relationships in the Fe–FeS–Co–CoS and Fe–Cr–S Systems*. Ph.D. thesis, Univ. of Wisconsin, Madison, Wisconsin.

WARD, J.C. (1970): The structure and properties of some iron sulphides. *Rev. Pure Appl. Chem.* **20**, 175-206.

WIESER, E., KRABBES, G. & TERUKOV, E.I. (1982): Detection of the metastable simultaneous occurrence of high- and low-temperature states in $Co_yFe_{1-y}S$ by Mössbauer spectroscopy. *Phys. Stat. Sol.* **A72**, 695-699.

WYSZOMIRSKI, P. (1976): Experimental studies of the ternary Fe–Co–S system in the temperature range 500–700°C. *Mineral. Pol.* **7**, 39-49.

_____ (1977): Phase relations in the Fe–Co–S system at 800°C. *Mineral. Pol.* **8**, 75-78.

Received August 8, 2001, revised manuscript accepted December 15, 2001.